Renewable and Sustainable Energy Reviews 15 (2011) 1228–1238

Contents lists available at ScienceDirect

Renewable and Sustainable Energy Reviews

journal homepage: www.elsevier.com/locate/rser

Hybrid solar cell based on blending of organic and inorganic materials—An overview

J. Chandrasekaran [a,*], D. Nithyaprakash [a], K.B. Ajjan [a], S. Maruthamuthu [a], D. Manoharan [a], S. Kumar [b]

[a] Department of Physics, Sri Ramakrishna Mission Vidyalaya College of Arts and Science, Coimbatore 641 020, Tamilnadu, India
[b] School of Environment, Resources and Development, Asian Institute of Technology, PO Box 4, Klong Luang, Pathumthani 12120, Thailand

ARTICLE INFO

Article history:
Received 2 June 2010
Accepted 9 September 2010

Keywords:
Bulk heterojunction
Organic/inorganic hybrid
Nanomaterials
Active layer
Power conversion efficiency

ABSTRACT

In recent years, increasing efficiency in organic solar cells is due to the bulk heterojunction concept. Hybrid solar cell (HSC) based bulk heterojunction is flourishing in the field of solar cell. This device is the combination of inorganic and organic materials. The efficacy of the power conversion efficiency has reached above 5% by following this combination method. This review provides general introduction, principle, working and characterization in the HSC involving the blend of organic/inorganic material as active layer. Different material combinations of the active layer and their performance are tabulated for better understanding of the HSC. This review ensures total compliance by discussing the fabrication technologies in terms of the HSC concept.

Contents

1. Introduction

Solar cells are designed to convert available light into electrical energy. They do this without the use of either chemical reactions or moving parts. Solar cells are usually made from silicon, the same material used for transistors and integrated circuits. The silicon is treated or "doped" in order to create charge carriers, so that when light strikes it electrons are released, leading to generation of electric current. The work of the French physicist Antoine – Cesar Becquerel in 1839 laid the founding stone for the development of solar cells. Becquerel discovered the photovoltaic effect while experimenting with a solid electrode in an electrolyte solution. He observed the development of voltage when light fell upon the electrode [1]. About 50 years later, Charles Fritts constructed the first true solar cells using junctions formed by coating the semiconductor selenium with an ultra thin, nearly transparent layer of gold. Fritts's devices were very inefficient, transforming less than 1% of the absorbed light into electrical energy [2,3]. By 1927 the transferring capacity of another metal-semiconductor junction solar cell, made of copper and the semiconductor copper oxide, had been demonstrated. Towards 1930 both the selenium cell and the copper oxide cell were being employed in light-sensitive devices, such as photometers for the use in photography. These early solar cells, however, still had energy-conversion efficiencies of less than 1%. This impasse was finally overcome with the development of the silicon solar cell by Russell Ohl in 1941. In 1954, American researchers, G.L. Pearson, Daryl Chapin, and Calvin Fuller, demonstrated a silicon solar cell having 6% energy conversion efficiency when used in direct sunlight [4,5]. By the late 1980's silicon cells, as well as those made of gallium arsenide,

* Corresponding author. Tel.: +91 422 2692461; fax: +91 422 2693812.
E-mail address: jchandaravind@yahoo.com (J. Chandrasekaran).

1364-0321/$ – see front matter © 2010 Elsevier Ltd. All rights reserved.
doi:10.1016/j.rser.2010.09.017

with efficiencies of more than 20% had been fabricated [6,7]. In 1989 the concentrator solar cell, a type of device in which sunlight is concentrated onto the cell surface by means of lenses achieved an efficiency of 37% owing to the increased intensity of the collected energy.

A broad range of solar cell technologies are currently being developed, including dye-sensitized, nanocrystalline photoelectron chemical solar cells, polymer/fullerene bulk heterojunctions, small molecule thin films and organic/inorganic hybrid solar cells. Hybrid solar cells are a mixture of nanostructures of both organic and inorganic materials. Therefore, they combine the unique properties of the inorganic semiconductor nanoparticle with those of the organic/polymeric materials [8]. It consists of p-type polymer semiconductor and an inorganic n-type material. Currently, the highest efficiency for such hybrid device has been obtained with CdSe nanoparticles and polythiophene.

In recent years, various solution processed bulk heterojunction photovoltaic devices have been reported using p-type conjugated polymers, in combination either with n-type polymers [9,10] or with fullerenes [11–14]. Alternatively conjugated polymers have been combined with n-type inorganic semiconductor nanoparticles. These hybrid polymers/inorganic nanoparticle bulk heterojunction can take advantage of the beneficial properties of both types of materials such as solution processing of polymer semiconductors and high electron mobility of inorganic semiconductors. So far, various hybrid polymer solar cells have been reported, using CdSe nanodots, nanorods [15] and tetrapods [16,17] and using of TiO_2 [18], ZnO [19,20], PbS [21,22], PbSe [23,24], $CuInS_2$ [25] and $CuInSe_2$ [26]. In a related approach nanostructured TiO_2 has been filled with conjugated polymers [27–32], but highest efficiency was recorded in the random mixtures of conjugated polymers and inorganic nanoparticles. In order to obtain hybrid polymer solar cells with high current and fill factor, both electron and hole mobilities must be optimized and most importantly balanced. Improvement of the performance of these devices is often sought in improving electron transport through inorganic component. In this paper, the researchers have focused only on HSC where organic and inorganic materials composites or blend are used, excluding tandem, dye and copolymer based cells.

2. Principle and working of hybrid solar cells

The developments of HSC's basic principle have been outlined. In HSC based on bulk heterojunction concept, the donor and acceptor are blended in single photovoltaic layer. The light induces electron transfer from the donor to the acceptor. The charge separation occurs throughout the active layer where the donor and acceptor are in contact. Once charge separation has occurred, the challenge to prevent the reverse process, recombination and delivering of charge to different electrodes occur. In these cells, transport of charge carriers to the electrodes and suppression of recombination are possible only if the donor and acceptor phases are completely ordered.

A complete hybrid solar cell is pictured in Fig. 1. The hybrid device generally has a transparent anode through which light enters. Conventional solar cells typically allow light to enter from the anode side while the anode itself consists of a grid of conductive material. The hybrid solar cells consist of at least four distinct layers, excluding the substrate, which may be glass. On the top of the substrate, the anode is laid. Indium tin oxide (ITO) is a popular anodic material due to its transparency and glass substrate coated with ITO is commercially available. A layer of the conductive polymer mixture PEDOT:PSS may be applied between anode and the active layer. The PEDOT:PSS layer serves in several functions. It not only serves as a hole transporter and exciton blocker, but it also smoothens the ITO surface, seals the active layer from oxygen, and keeps the anode material from diffusing into the active layer, which can lead to unwanted trap sites. Next, on the top of the PEDOT:PSS, an active layer is deposited which holds the responsibility for light absorption, exciton generation/dissociation and charge carrier diffusion. The active layer is made up of two materials namely donor and acceptor. Polymers are the common donors whereas nanoparticles act as common acceptors. Cathode, typically made of Al, Ca, Ag and Au was coated on top of the active layer

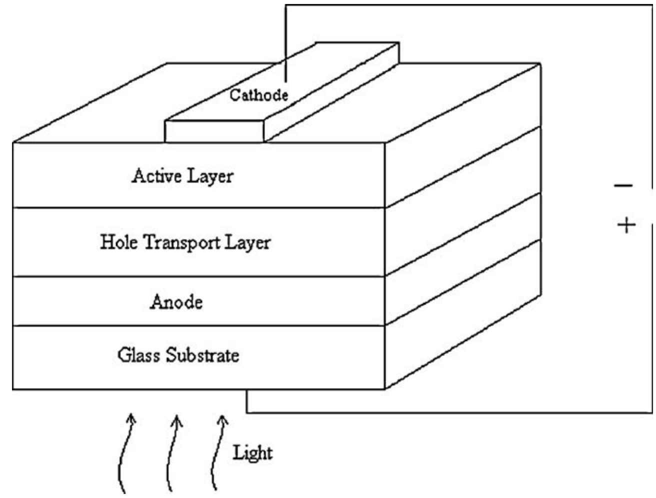

Fig. 1. Structure of hybrid solar cell.

The *I–V* characterization of the hybrid solar cell device is shown in Fig. 2. In the dark, *I–V* curve passes through the origin indicating the absence of potential and current. But when the device is exposed to light, the *I–V* curve shifts downwards.

3. Characterization of hybrid solar cell

The following terms are often used to characterize solar cells, some items are also shown in the *I–V* graph:

(i) **Air mass**: It is the ratio of the path length of the sun rays through the atmosphere when the sun is at a given angle θ to the zenith. An air mass distribution of 1.5, as specified in the standard condition, corresponds to the spectral power distribution observed when the sun's radiation is coming from an angle to over head of about 48°.

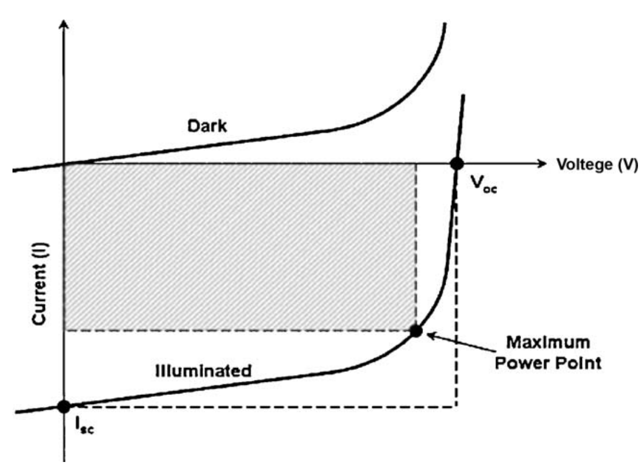

Fig. 2. *I–V* characteristics of hybrid solar cell.

Table 1
Review of hybrid solar cell based on blending of organic and inorganic materials.

S. No.	Author's name	Aim of the work	Experimental details	Author's remarks
1	Elif Arici et al. (2003)	Characterizing HSC based on nanoparticles of $CuInS_2$ inorganic matrices.	The device structure used was: (a) ITO/PEDOT:PSS/CIS/LiF/Al (b) ITO/PEDOT:PSS/CIS/PCBM/LiF/Al (c) ITO/CIS:PEDOT:PSS/LiF/Al (d) ITO/CIS:PEDOT:PSS blend/PCBM/LiF/Al.	In BHJ device (d) PCE was high (0.07%) compared to single layer device (c) (0.003%) [33].
2	Waldo J.E Beek et al. (2004)	Fabricating HSC from ZnO nanoparticles and a conjugated polymer.	The structure of the cell was glass plate/ITO/PEDOT:PSS/MDMO-PPV:nc-ZnO blend/Al layer.	A PCE of 1.6% (0.71 sun equivalent) and 1.4% (1.7 sun equivalent) was obtained for the blended hybrid solar cell which illustrated the effectiveness of using a combination of organic and inorganic materials for photovoltaic applications [19].
3	Elif Arici et al. (2004)	Investigating blends of polyhexylthiophene (P3HT) with copper indium diselenide nanocrystals for photovoltaic applications.	The cell structure was ITO/CISe:P3HT blend/Al. Blends of CISe/P3HT have been prepared by varying the amount of the CISe in the films.	Films consisting of TOPO-capped CISe:P3HT in a weight ratio of 6:1 showed a significantly better photovoltaic response in comparison with a P3HT single layer [34].
4	Jinsong Liu et al. (2004)	Fabricating HSC using polythiophene and ncs of CdSe.	The device structure of the cell was ITO/PEDOT/P3HT:CdSe ncs/Al.	The end functional P3HTenhanced the performance of P3HT: CdSe SC by increasing the dispersion of CdSe ncs without introducing insulating surfactants [35].
5	Waldo J.E. Beek et al. (2005)	Preparing HSC using zinc oxide precursor and conjugated polymer.	The fabrication process was ITO coated plate/PEDOT:PSS/MDMO-PPV and ZnO blend/Al. Annealing and drying were carried out in a perfect manner.	The PCE of 1.1% was reached for the use of precursor ZnO device, and for ZnO np:MDMO-PPV blend it was 1.6%, but V_{oc} was found to be increased for the cell with precursor ZnO device [36].
6	Lenneke H. Slooff et al. (2005)	Investigating the influence of relative humidity on the performance of polymer/TiO_2 PV cells.	The bilayer and BHJ device with structure of ITO/TiO_2/MDMO-PPV/PEDOT:PSS/Au and ITO/PEDOT:PSS/MDMO-PPV:TiO_2 blend/LiF/Al was fabricated for comparison.	The bilayer device showed PCE was 0.3%. In BHJ the RH during spin coating strongly influenced the TiO_2 structure and the device performance. Generally BHJ gives higher efficiency than a bilayer. But in the case of BHJ efficiency was low owing to a lack of crystalline in the TiO_2 [37].
7	P.Y. Stakhira et al. (2005)	Investigating the electrical and photovoltaic property of PAN–InSe composites.	The active materials used were SnO_2/PAN–InSe composite/Au. Volt–ampere characteristics of the structure were described by Shockly equation.	The experiment proved that the *V–I* characteristic PAN/p-type InSe micro particle exhibited rectifying junction behavior and the proposed structure showed a nonlinear dependence of current with light intensity [38].
8	Andrew A.R. Watt et al. (2005)	Fabricating polymer solar cell using PbS nanocrystal.	The cell was with a structure of ITO glass/PEDOT:PSS/PbS:MEH-PPV composite/Al.	PCE for white light and single wavelength was observed to be 0.7% and 1.1% [39].
9	Yi-Jun Lin et al. (2006)	Investigating organic–inorganic hybrid materials based on the P3MeT and TiO_2.	P3HT was coated on the top of P3MeT/TiO_2/ITO. Al was used as top electrode by the evaporation deposition of 60 nm thick.	The PCE of the photovoltaic solar cell was $3.22 \times 10{-}3\%$. The efficiency was low owing to poor contact between polymer and TiO_2 [40].
10	Serap Gunes et al. (2006)	Fabricating HSC using HgTe nc and nanoporous TiO_2 electrodes.	ASOS device was fabricated following the structure ITO/nanoporous TiO_2/HgTe-AS/ncs HgTe-OS:P3HT/Au. Reference device AS was prepared in identical manner but with only HgTe-AS nc on nanoporous TiO_2 and without HgTe-OS in P3HT. Reference OS was made with HgTe-OS ncs in polymer blend but without HgTe-AS ncs on the nanoporous TiO_2 surface and Reference NO device was prepared without nanocrystal.	HgTe ncs were found to be optically active both in OS and AS device. It also helps to reduce the interfacial charge carrier recombination at nanoporous TiO_2 interface. ASOS device performance was found to be higher than AS, OS and NO device [41].
11	Waldo J.E. Beek et al. (2006)	Investigating HSC from regioregular polythiophene and ZnO nanoparticles.	The exact blends of ZnO and P3HT were made and spin casted on glass plate coated with ITO and PEDOT:PSS respectively followed by depositing Al by means of thermal evaporation.	PCE of 0.9% was obtained for this type of cell. Further improvement in the polymer chain or nanoparticles can enhance the performance [42].
12	Sang-Hyun Choi et al. (2006)	Synthesis of size-controlled CdSe quantum dots and characterization of CdSe-conjugated polymer blends for hybrid solar cells.	Size controlled CdSe Q-dots were synthesized by wet chemical method. PEDOT:PSS was spin coated on ITO followed by CdSe Qdots-P3HTand CdSe Q dots-MEH-PPV polymer solution containing 1–8 vol% of pyridine–chloroform. Al was used as working electrode.	The hybrid solar cells made of CdSe Qdots-P3HT polymer blends with the pyridine–chloroform solvent mixture could achieve power conversion efficiencies of about 0.05%. It was also confirmed that binary solvent mixtures play an important role in the fabrication for hybrid solar cells [43].

13	Yi Zhou et al. (2006)	Investigating the effect of nc composites on the PV properties of the SC.	Tetra podal $CdSe_xTe_{1-x}$ nc with different compositions was synthesized. ITO/PEDOT:PSS/CdSe, $CdSe_xTe_{1-x}$ and CdTe ncs were mixed with MEH-PPV to form different structures/Al. The PCE was recorded for different wt ratios of CdSe:MEH-PPV.	The optimal blend ratio of CdSe:MEH-PPV with 9:1 showed the highest PCE of 1.13% [44].
14	Lili Han et al. (2006)	Fabricating hybrid solar cells based on zinc-blend CdSe ncs/MEH-PPV.	ITO was spin coated with PEDOT:PSS. The CdSe ncs were dissolved in a mixture of pyridine. Two master solutions of MEH-PPV and CdSe ncs were mixed in desired ratios and the blended films with desired thickness were spin coated on top of the dried PEDOT:PSS. Finally, the Al cathode was thermally deposited on top of the blended film.	The photovoltaic cell obtained from the spherical zinc-blend CdSe ncs with MEH-PPV reached an energy conversion efficiency of over 0.85% [45].
15	L. Jan Anton Koster et al. (2006)	Studying the transport properties of blend MDMO-PPV/ZnO and identifying the factors affecting the performance of the cell.	The material used for the fabrication was ITO/PEDOT-PSS/MDMO-PPV/nc-ZnO/LiF/Al. By changing the ratio of MDMO-PPV/ZnO as 1:2 and 2:1 hole only and electron only devices were fabricated by suppressing electrons and holes respectively. The *J–V* characteristic was studied.	The transport of charge carrier in MDMO-PPV and nc-ZnO by selectively suppressing the injection of one of the charge carrier was studied.The hole mobility in the polymer phase of MDMO-PPV/nc-ZnO (1:2 by wt) was found to be equal to the mobility in prestine MDMO-PPV. It was found that the hole mobility was not affected by the ZnO. By replacing MDMO-PPV with a polymer of higher hole mobility which combines with ZnO, higher efficiency solar cells can be fabricated. Efficiency of 1.6% was obtained [46].
16	Seok-Soon Kim et al. (2007)	Comparing the PV performance of hybrid solar cells based on different nanostructures using TiO_2 and MEH-PPV.	The solar cells with a structure of flat TiO_2 electrode, random TiO_2 np network and 2D TiO_2 nanostructure were fabricated.	High efficiency (0.21%) was obtained for PV based on ordered 2D TiO_2 nanostructure owing to improved charge transport and separation with large interfacial area [47].
17	Date J.D. Moet et al. (2007)	Studying the limitation of HSC from mixture of dialkoxy-substituted PPV with precursor ZnO owing to partial degradation of the polymer during processor.	The device structure used was ITO/PEDOT/PSS/Active layer (MDMO-PPV:ZnO)/LiF/Sm/Al. The fabrication was also made with P3HT:ZnO as active layer for comparison.	The presence of highly reactive diethylzinc during processing of BHJ of MDMO-PPV and ZnO caused the polymer to degrade. HSC based on P3HT and ZnO had an estimated PCE of 1.4% [48].
18	Li Wang et al. (2007)	Fabricating multiarmed CdS nrs/MEH-PPV HSC.	ITO coated glass was spin coated with the mixed solution of MEH-PPV and nc-CdS followed by thermal evaporation of Al. The active layer was processed in the solution of pyridine and chlorobenzene.	Higher efficiency was obtained with pyridine (0.89%) than with chlorobenzene (0.14%). Thermal treatments of the blend further enhanced the efficiency to 1.17% [49].
19	Zhijie Wang et al. (2008)	Fabricating MDMO-PPV capped PbS Q-dots solar cell.	Blending of MDMO-PPV with MDMO-PPV capped PbS Q-dots as the active layer between anode (ITO) and cathode (Al) and solar cells with different annealing process were also discussed.	The highest energy conversion efficiency (0.013%) with the structure of ITO/PEDOT:PSS/MDMO-PPV/MDMO-PPV capped PbS Q-dots/Al was obtained [50].
20	Li Yan et al. (2008)	Investigating the PV properties of MEH-PPV/TiO_2 nanocomposites.	The structure of the cell followed was ITO/PEDOT:PSS/MEH-PPV:TiO_2 (nps and nts respectively)/Al.	MEH-PPV:TiO_2 nanotubes had better PV properties than MEH-PPV:TiO_2 nanoparticles [51].
21	P. Suresh et al. (2008)	Investigating the optical and photovoltaic properties of HSC based on blend of PPHT:ZnO and PPHT:dye:ZnO.	The solar cell was fabricated as follows ITO/PPHT:ZnO/Al and also PPHT:ZnO prepared in different solvent.	The efficiency of the solar cell 0.12% and 0.55% for PPHT:ZnO and PPHT:dye:ZnO respectively was obtained, which enhances the photon absorption in visible region. Increase in absorption and FL quenching owing to incorporation of dye in PPHT:ZnO composite was noticed. The effect of solvent used for PPHT:ZnO layer was also studied [52].
22	Mingqing Wang et al. (2008)	Fabricating of PPV/TiO_2 hybrid composites from PPV precursor reaction in aqueous media.	The structure of the solar cell was ITO/PEDOT/PPV/TiO_2/Al. TiO_2 introduced situ sol–gel approach and direct mixing method was adopted.	In sol–gel method TiO_2 nanocomposites (40 wt%) efficiency was high (0.018%) compared to direct mixing. The sol–gel method can be attributed to the nanosized phase separation and direct mixing attributed to the increase of the aggregation [53].

Table 1 (*Continued*)

S. No.	Author's name	Aim of the work	Experimental details	Author's remarks
23	K. Vandewal et al. (2008)	Studying two modes of FTPS for a fast and highly sensitive spectral characterization of organic and HSC.	(i) P3HT, PCBM and P3HT:PCBM active layers were coated on to the PEDOT:PSS layer which was spin coated onto ITO glass. Al was the top electrode.	The FTPS technique detected sub-band gap optical transition. In P3HT:PCBM blend, the sub-band gap absorption is dominated by formation of a ground state charge transfer complex and no light could be detected.
			(ii) An aqueous citraperoxo – Ti(IV) gel precursor was spin coated onto FTO. After 650 °C heat treatment, TiO_2 was formed. P3HT layer was spin coated on top to form 2 wt%. Gold act as the top electrode.	The detected low energy bands in pure P3HT and in P3HT/TiO_2 junctions appeared after irradiation with $E > 1.9$ eV [54].
24	Yi-Ming Chang et al. (2008)	Introducing hydroxyl moiety onto P3HT to promote polymer titanium interaction.	The photovoltaic device was prepared by spin coating PEDOT:PSS on ITO coated glass or PET substrate, then the photoactive layers P3HT:TiO_2, P3HT-OH:TiO_2 and P3HT:P3HT-OH:TiO_2 hybrid solution was spin coated on the top of PEDOT:PSS. Al was used as electrode.	P3HT:P3HT-OH:TiO_2 was found to be more efficient than P3HT:TiO_2 and P3HT-OH:TiO_2 [55].
25	Frederik C. Krebs et al. (2008)	Fabricating a nanostructured polymer solar cell which operates in air.	ITO glass was spin coated with ZnO and the active material used was P3CT/ZnO (P3CT was obtained from P3MHOCT). PEDOT:PSS and Ag were used as the top electrodes. The experiment was performed in inert and atmospheric conditions.	The morphology of the device films and materials characterized by TEM and X-ray scattering techniques, showed that the particles were well dispersed and quite homogeneous with respect to particle size. The device performance was found to improve in atmosphere [56].
26	Steven K. Hau et al. (2008)	Improving the stability by reversing the nature of charge collection using ZnO as electron selection layer.	ITO was coated on glass and plastic for comparison. Two types of device were fabricated conventional device ITO glass/PEDOT:PSS/P3HT:PCBM/LiF/Al and inverted SC ITO glass/ZnO/P3HT:PCBM/PEDOT:PSS/Ag.	The devices fabricated from the ZnO nps on ITO-coated glass had an average PCE of 3.6%, which was very similar to that obtained from the high temperature processed sol–gel devices [57].
27	I. Haeldermans et al. (2008)	Forming charge transfer complex (CTC) in P3HT:TiO_2 BHJ SC.	The active device was prepared with ITO/PEDOT:PSS/P3HT:TiO_2/Ca/Al. The active layer P3HT:TiO_2 was prepared with various vol% of TiO_2. Similar fabrication was made with ZrO_2.	In the case of the P3HT:TiO_2 blend, the energy of the CT state was lower than both the band gaps of P3HT and TiO_2, which implied that in this case, the CT state may be efficiently populated. In P3HT:ZrO_2 blends, however, the CT state was higher in energy than the P3HT excitonic state, resulting in poor carrier generations [58].
28	Johann Boucle et al. (2008)	Investigating BHJ SC based on TiO_2 nr and P3HT.	Blend film of TiO_2:P3HT was spin coated onto glass substrate followed by PEDOT:PSS. Al or Au was used for top metallic contact. The device structure for direct polarity was ITO/PEDOT:PSS/blend/Al and for reverse polarity ITO/dense TiO_2/blend/PEDOT:PSS/Au.	Compared with the direct polarity where the ITO electrode was used to collect holes, the reverse geometry used the dense TiO_2 and PEDOT:PSS layers as hole and electron blocking layers respectively resulting in improved selectivity [59].
29	Serap Gunes et al. (2008)	Fabricating surface modified TiO_2 np with 6PAA.	The cell structure was ITO/PEDOT:PSS/TiO_2:P3HT (with different ratio)/LiF/Al. TiO_2 nps surface was modified with 6PAA.	As the ratio of P3HT:TiO_2/6PAA decreases, the current increases slightly [60].
30	Jincheng Liu et al. (2008)	Studying MEH-PPV/TiO_2 HSC using different ligands.	The device structure was ITO/PEDOT:PSS/blend of MEH-PPV and TiO_2 nrs/Al.TiO_2 was capped with different ligands OLA, OPA and TP.	TiO_2 capped with TP resulted in higher PCE of 0.157%, proving to be one of the best ligands for fabrication of HSC [61].
31	Qiquan Qiao et al. (2008)	Preparing HSC using buffer layer from water solution processing.	The structure of the device was FTO/TiO_2 buffer layer/TiO_2/PTEBS blend/Au. The blend of the active layer was done in water.	A titanium buffer layer was introduced into an all water solution based BHJ polymer SC to improve interfacial contact. The efficiency improved was quadrupled (0.04–0.17%) [62].
32	Michael Bredol et al. (2009)	Preparing hybrid SC with ZnS nanoparticles and polymer.	The active layers of P3HT/ZnS:Mn blend (without ZnS np and with 17 and 50 wt% of ZnS np) were spin coated on ITO glass substrate with PEDOT:PSS. Al was deposited as top electrode.	*I–V* characteristic of a device with nanoparticles content of 50 wt% reached a very high power conversion efficiency of 0.2% compared to 17 wt% and without ZnS nanoparticles [63].
33	Tsung-Wei Zeng et al. (2009)	Studying the performance of P3HT with semiconductor TiO_2 nanorods for use in polymer solar cell.	The structure of ITO/PEDOT:PSS/P3HT:TiO_2 nanorods/TiO_2 nanorods/Al was followed.	PV performance having 0.83% PCE was obtained owing to high molecular weight P3HT, High boiling point solvent trichlorobenzene and pyridine-modified TiO_2 nanorods [64].

34	Lung-Chein Chen et al. (2009)	Investigating the influence of dopant and polymeric matrix on ITO/p-ZnPc/n-Si HSC.	ITO was coated on the glass to form anode substrate. On n-type Si substrate, ZnPC + PMMA + I_2 were deposited. These substrates were sandwiched between cathode material Al and anode. Different devices replacing iodine by aluminum chloride hexahydrate, Magnese chloride and indium chloride tetrahydrate were fabricated and results were compared.	PCE of 5.55% was obtained for the I_2 based devices due to the highest absorbance and the lowest absorption edge exhibited by I_2 doped ZnPC film at about 3.3 eV [65].
35	Ming-Chung Wu et al. (2009)	Studying the effect of molecular weight of P3HT and performance of P3HT:TiO_2 nanorods by scanning probe microscope.	The solar cell was fabricated with structure ITO/PEDOT:PSS/P3HT:TiO_2 nanorods/Al.	The device efficiency (0.61%) was improved by increasing the molecular weight (66 kDa) of P3HT due to the increase in both light harvesting and carrier mobility [66].
		Comparing device performance by varying PMMA concentration is P3HT:TiO_2 active layer.	The cell with a structure of ITO/PEDOT:PSS/P3HT/varying concentrations of PMMA:TiO_2 nanorods/Al was fabricated.	The solar cell performance with PMMA concentrations of (0.0, 1.6, 3.2, and 11.6 wt %) were studied and it showed high PCE of (η = 0.65%) for 1.6 wt% PMMA concentration is the active layer in P3HT/PMMA:TiO_2 blends [67].
36	Daqin Yun et al. (2009)	Comparing the performance of solar cell based on MOPPV–ZnSe with and without incorporation of PbSe nano crystal structure.	The solar cell was fabricated with a structure of ITO/PEDOT:PSS/MOPPV–ZnSe/with and without PbSe/Al.	Improved device performance was obtained by incorporation of PbSe Q dots in active layer with PCE of 0.14% [68].
37	Zhijie Wang et al. (2009)	Fabricating the HSC by using SnS nanoparticle.	The hybrid device structures of ITO/PEDOT:PSS/P3HT:SnS/Al and ITO/PEDOT:PSS/MDMO-PPV:SnS/Al were fabricated for comparison.	In P3HT based solar cells with 86 wt% SnS had good efficiency (0.01%) and MDMO-PPV with 67 wt% SnS proved an efficiency of 0.02% [69].
		Fabricating the HSC MDMO-PPV capped PbS nanorods.	The solar cell was fabricated with a structure of ITO/PEDOT:PSS/MDMO-PPV:PbS nanorods/Al.	The solar cell performance was optimized and the influence of ambience, annealing process and nanorods content was analysed. 75 wt% PbS content solar cell offered the best performance compared to others [70].
38	Chin-Yi Liu et al. (2009)	Fabricating the HSC based on blends of Si ncs and P3HT.	The solar cell was fabricated with structure ITO/PEDOT:PSS/Si ncs:P3HT/Al.	The Si ncs size decreased with increasing PV properties. Roughly 35 wt% of Si ncs produced the best PV devices with 1.15% PCE [71].
39	Chen-Yu Chou et al. (2009)	Studying the lengthening of solidification time to improve PCE of polymer/ZnO nanorod HSC.	The structure of the solar cell was ITO/ZnO film/ZnO nanorod/P3HT:PCBM/Ag.	For the longest drying time of the device PCE (3.58%) was high compared to fast dried device, owing to crystallinity of the polymer and infiltration of the photo active layer [72].
40	Golap Kalita et al. (2009)	Demonstrating hybrid solar cells using Si nws and polymer incorporating MWNTS.	Silicon nanowires were fabricated on Si wafer. P3OT and P3OT:OMWNTS were drop casted over nanowires. Au was used as working electrode.	The incorporation of functionalized MWNTs along with the polymers showed considerably enhanced device performance owing to improved hole mobility. The fabricated device with the structure Au/P3OT + O-MWNTs/n-Si nws marked a conversion efficiency of 0.61% [73].
41	Yun-Yue Lin et al. (2009)	Demonstrating red light harvesting owing to P3HT/FeS_2 nanocrystal.	The structure of HSC was ITO/PEDOT:PSS/P3HT:FeS_2 hybrid/Al.	The PCE of the device was 0.16%. The result demonstrated that the adding of FeS_2 ncs in P3HT can contribute to the extended photovoltaic response in the red light region, which can act as a potential candidate for the polymer/inorganic hybrid solar cell application [74].
42	Deepak Verma et al. (2009)	Studying the characteristics of blend solution having proper dispersion of surfactant free CdTe np with MEH-PPV.	The active materials used were ITO/PEDOT:PSS/CdTe/MEH-PPV/Al. Spin coating technique was used. CdTe and MEH-PPV were taken in different ratios for the study.	The hybrid layers deposited with CdTe and MEH-PPV with weight ratio 40:3 indicated proper dispersion of nanoparticles and proved higher PCE of 0.06% [75].
43	Akihiro Takeda et al. (2009)	Investigating Cd free inorganic hybrid solar cells with $CuInS_2$ and C_{60}.	Bilayer and BHJ cells were fabricated using CIS and C_{60} as active layer as follows: FTO glass/PEDOT:PSS/CIS/C_{60}/Al and FTO glass/PEDOT:PSS/CIS:C_{60}/Al.	The efficiency of BHJ proved to be Higher (8×10^{-4}) than bilyer (6×10^{-4}) owing to increase in photoelectron conversion area [76].
44	Junpeng Liu et al. (2009)	Demonstrating HSC based on vertically oriented ZnO nws and organic molecular materials.	Devices are fabricated with different ZnO nw diameter, length and organic layer thickness ITO/ZnO/ZnO nw/CuPC:C_{60}/CuPc/PEDOT:PSS/Au.	The efficiency was found to increase by incorporating ZnO nws. The PCE was maximum for a device with smaller thickness 20 nm diameter and length 100 nm which had enough space to allow the organic layers to infiltrate the space between the ZnO nws. The PCE was 0.53% [77].

Table 1 (*Continued*)

S. No.	Author's name	Aim of the work	Experimental details	Author's remarks
45	Vladimir Svrcek et al. (2009)	Investigating the photoelectric property of BHJ SC based on Si-ncs and P3HT.	Two different studies were made to analyse photoconductivity property of BHJ: (a) Parallel conductivity was investigated using Si-ncs/P3HT blend coated on platinum contact evaporated on glass. (b) For perpendicular conductivity materials used in fabrication were TCO coated glass/PEDOT:PSS/Si-ncs:P3HT/TiO_2 nts. Si-ncs/P3HT blend was incorporated into TiO_2 nts.	*I–V* characteristic enhanced when BHJ was introduced into TiO_2 nt. The arrangement of Si-ncs/P3HT BHJ within ordered TiO_2 nt perpendicular to the contact facilitated excition separation and charge transfer along nts [78].
46	Alejandro L. Briseno et al. (2010)	Demonstrating the SC based on P3HT and QT with ZnO single nw.	The device was fabricated using Pristine ZnO, ZnO/P3HT composites and ZnO/QT composite.	Oligo and polythiophene were grafted onto ZnO nw to produce p–n heterojunction. The efficiency of ZnO/P3HT composite was found to be high (0.036% compared to other devices [79].
47	Smita Dayal et al. (2010)	Fabricating BHJ SC with CdSe tetra pods and low band gap polymer.	ITO coated glass was coated with PEDOT-PSS followed by spin coating the active layer CdSe:PCPDTBT (9:1 wt. ratio). Al was used as the working electrode.	BHJ solar cell of 3.13% was obtained. Low band gap polymer played an important role for better solar spectrum harvesting and contribution of np towards achieving high PCE [80].
48	Kaushik Roy Choudhury et al. (2010)	Demonstrating solution processed hybrid polymer nc-IR LEDs with enhanced efficiency using PbSe ncs in polymer.	PEDOT:PSS was spin coated onto ITO glass with active layer prepared with blend of PbSe ncs and MEH-PPV in cholorobenzene in various proportions. BCP was thermal evaporated on active layer followed by evaporation of LiF/Al.	Investigation of the optimizated device based on nanocomposites blend architecture was achieved with maximum EQE of 0.83% at a peak emission wave length of 1280 nm [81].
49	Tzong-Liu Wang et al. (2010)	Investigating electrochemical and photochemical properties of HSC using CdSe–PVK composite.	ITO/PEDOT:PSS/active layer P3HT:CdSe-OH or P3HT:CdSe–PVK (1:1 wt ratio)/Al were the device structure.	The performance of the device P3HT:CdSe–PVK blend was found to be significant in composition with P3HT:CdSe–OH showing efficiency of 0.02% [82].
50	Jun Yan et al. (2010)	Electropolymerizing PEDOT:PSS films on ITO glass in BFEE with three electrode system.	ITO/PEDOT/ZnO:MDMO-PPV 1:2 ratio/Al. PEDOT was prepared with electrolysis of trielectrode where pt acts as counter electrode, ITO glass as working and Ag/AgCl electrode as reference electrode. ITO and Ag/AgCl were kept parallel in the cell during polymerization process. The electrolytic solution was EDOT in BFEE.	Electrochemical polymerization process gave higher conversation efficiency (0.33%) when compared to the spin coating technique [83].
51	Minas M. Stylianakis et al. (2010)	Modifying of SWCNT with thiophene.	ITO substrate was coated with PEDOT:PSS followed by spin coating of three different photoactive layers (a) P3HT–PCBM (b) SWCNT doped P3HT:PCBM/P3HT:PCBM and (c) SWCNT-CONHTh doped P3HT:PCBM Al was used as electrode.	Modified SWCNT was incorporated, which contains pendant thiophene rings into polymer/fullerene PV device. Polymer/fullerene cell with SWCNT CONHTh was found to be superior to other devices achieving the efficiency 1.78% owing to an extention of the excition, dissociation area and to faster electron transfer than nt [84].

(ii) **Open-circuit voltage (V_{oc})**: When the cell is operated at open circuit, $I = 0$ and the voltage across the output terminals is defined as the open-circuit voltage.

$$V_{oc} = \frac{kT}{q} \ln\left(\frac{I_L}{I_0} + 1\right)$$

(iii) **Short-circuit current (I_{sc})**: When the cell is operated at short circuit, $V = 0$ and the current I through the terminals is defined as the short-circuit current.

$$I_{SC} \approx I_L$$

(iv) **Maximum power point (MPP)**: (I_{mpp}, V_{mpp}) on the I–V curve is the point where maximum power is produced. Power (P) is the product of current and voltage ($P = IV$) and is illustrated in the Fig. 2 as the area of the rectangle formed between a point on the I–V curve and the axes. The maximum power point is the point on the I–V curve where the area of the resulting rectangle is largest.

(v) **Fill factor (FF)**: This is the ratio of the maximum power point to the product of open circuit voltage (V_{oc}) and the short circuit current (I_{sc}):

$$FF = \frac{P_m}{V_{OC} \times I_{SC}} = \frac{\eta \times A_C \times E}{V_{OC} \times I_{SC}}$$

(vi) **Power conversion efficiency (PCE or η_e)**: The ratio of power output to power input. In other words, PCE measures the amount of power produced by a solar cell relative to the power available in the incident solar radiation (P_{in}). P_{in} here is the sum over all wavelengths and is generally fixed at 1000 W/m^2 when solar simulators are used.

$$\eta_{AM1.5} = \frac{P_{OUT}}{P_{IN}} = FF\frac{V_{OC}I_{SC}}{P_{IN}}$$

(vii) **Quantum efficiency (QE)**: It refers to the percentage of photons that are converted into electric current (i.e., collected carriers) when the cell is operated under short circuit conditions.

- **External quantum efficiency**: External quantum efficiency (EQE) is the fraction of incident photons that are converted to electrical current, while internal quantum efficiency (IQE) is the fraction of absorbed photons that are converted to electrical current.
- **Internal quantum efficiency**: Internal quantum efficiency is related to external quantum efficiency by the reflectance (R) and the transmittance (T) of the solar cell by

$$IQE = \frac{EQE}{(1 - R - T)}$$

4. Review of hybrid solar cell

This review aims to summarize the recent approaches to fabricate the HSC in different combinations of organic and inorganic materials and their efficiency. In this article a total of 84 papers have been referred to, among which 53 have been summarized in Table 1, in terms of names of authors' (reference), aims of their works, approaches to their works (materials used/ experimental details) and authors conclusions (reports). The essence of this analysis will be a delightful treat for the budding researchers in order to understand HSC.

5. Results and discussion

The above details lead to the following discussion:

Anode material used is glass or plastic coated with either of ITO, FTO, GZO, etc., but in general ITO coated glass is mostly used owing to its stability. PEDOT:PSS is the often used hole transporting layer, but a few researchers have used TiO_2 as charge transport complex (CTC) acting as an intermediate state in charge separation and recombination in order to enhance the device performance. PEDOT is another material used for the same purpose. In the active layer many works have been carried out. The following are the points to be noted.

1. Lower band gap polymers with a broad absorption spectrum increases PCE owing to higher solar spectrum harvesting.
2. Incorporating CdSe np enhances the thermal stability of PVK.
3. Chemical combination of single or multiwalled CNT, addition of ZnO nws incorporated into polymer attributes to an extension of excitation dissociation area and a faster electron transfer.
4. Addition of FeS_2 ncs in P3HT extends the PV response in red light region.
5. Introduction of optical spacers like TiO_x invole multiple reflection leading to higher performance.
6. Lengthening of solidification time of active layer increases the PCE.

In general many cathode materials were used but Al was the mostly preferred one. Some researchers worked with optimized weight ratio of the donor and acceptor, suitable solvent for blending of the active layer, changing the different electrode and varying the donor or acceptor concentration. Many experimental comparative works have been done between BHJ and bilayer device.

In the hybrid solar cells polymer materials acting as donors are P3HT, PPHT, P3OT, P3BT, MDMO-PPV, MEH-PPV, MOPPV etc., and inorganic materials used as acceptors are TiO_2, ZnO, PbS, ZnS, CdS, SnS, CIS, PbSe, CuPc, PS, Si nws, Si ncs, etc. Among these donors and acceptors, P3HT proved to be one of the best donors and TiO_2, ZnO and Si acted as good acceptors. By reversing the nature of charge collection using ZnO as an electron selection layer [57], lengthening of solidification time [72], using I_2 dopants [65], CdSe tetrapodes and low band gap polymer [80] higher efficiency can be achieved.

6. Conclusion

Increasing consumption of electric power and effect of global warming have deviated researchers towards alternative pollution free natural sources from fossil fuels. One such field of conversion of solar energy into electric energy plays a vital role in research, technology and domestic power consumption. Efforts in the last decade have led to number of new technologies to increase the efficiency. One such grown field is the hybrid solar cell in particular, where blend of organic/inorganic is used for charge separation. The various methods of blending, using nanotubes or nanoparticles, have raised the performance of the cell. Different techniques of coating active layers change the morphology, which, in turn, affects the conversion output. Use of buffer layers and optical spacers further enhances the efficiency. The focus of the recent research on this blending technique of active layers has raised the cell efficiency above 5%. This review helps in the further improvement of the device performance for the selection of suitable material with proper band gap and knowing other factors that affect efficiency.

Acknowledgement

The two of us (J.C and D.N) gratefully acknowledge the financial support from the UGC, Government of India for the major research project (F-33-19/2007(SR)).

Appendix A

A_c	Surface area of the solar cell
AFM	Atomic Force Microscopy
Ag	Silver
Al	Aluminium
AS	Aqueous soluble
Au	Gold
BCP	Bathocuprine
BFEE	Boron trifluoride diethyl etherate electrolyte
CdSe	Cadmium selenide
CIS	Copper indium sulfide
CISe	Copper indium diselenide
CT	Charge transfer
$CuInS_2$	Copper indium sulfide
CTC	Charge transport complex
E	Input light irradiance
ECE	Energy conversion efficiency
EDOT	3,4-Ethylenedioxythiophene
FeS_2	Iron disulphide
FL	Fluorescence
FTPS	Fourier-Transform Photocurrent Spectroscopy
FTO	Fluorine doped tin oxide
HgTe-AS	Mercury telluride – aqueous soluble
HgTe-OS	Mercury telluride – organic solvent
HSC	Hybrid solar cell
I_L	Photogenerated current (A)
I_0	Reverse saturation current (A)
I_2	Iodide
IR LED	Infra red light emitting diode
ITO	Indium tin oxide
k	Boltzmann's constant
LiF	Lithium fluoride
MDMO-PPV	Poly[2-methoxy-5-(3′7′-dimethyloctyloxy)-1,4-phenylene vinylene]
MEH-PPV	Poly[(2-methoxy-5-(2′-ethyl-hexyloxy)-1,4-phenylene) vinylene]
Mn	Manganese
MOPPV	Poly(2-methoxy,5-octoxy)-1,4-phenylene vinylene
MWNTS	Multi-walled carbon nanotubes
nc	Nanocrystalline
np	Nanoparticle
nr	Nanorod
nt	Nanotube
nw	nanowire
OLA	Oleic acid
OPA	Octyl-phosphonic acid
OS	Organic solvent
P_m	Maximum power point
PAN	Polyaniline
PANI	Polyaniline
P3CT	Poly(3-carboxydithiophene)
P3HT	Poly(3-hexylthiophene)
P3MeT	Poly(3-methylthiophene)
P3MHOCT	Poly-(3-(-methylhexan-2-yl)-oxy-carbonyldithiophene)
P3OT	Poly(3-octylthiophene)
PMMA	Poly(methyl methacrylate)
PCE	Power conversion efficiency
PCBM	(a) 1-((3-methoxycarbonyl)-prop-1-yl)-1-phenyl (6,6) C_{61}; (b) [6,6]-phenyl-C_{61}-butyric-acid methyl ester
PCPDTBT	Poly(2,6-(4,4-bis-(2-ethylhexyl)-4H-cyclopenta (2,1-b; 3,4-b′) dithiophene)-alt-4,7-(2,1,3-benzothiadiazole))
PEDOT:PSS	Poly(3,4-ethylenedioxythiophene):poly(styrenesulfonate)
PPHT	Poly-3-phenyl hydrazones thiophene
PTEBS	Poly[2-(3-thienyl)-ethoxy-4-butylsulfonate]
PV	Photovoltaic
PVK	Poly-vinyl carbazole
q	Elementary charge
Q-dots	Quantum dots
QT	Quarterthiophene
RH	Relative humidity
Sm	Samarium
SnO_2	Tin oxide
SnS	Tin sulfide
SWCNT	Single walled carbon nano tubes
T	Absolute temperature
TCO	Transparent conductive oxide
TiO_2	Titaniumdioxide
TOPO	Trioctylphosphine oxide
TP	Thiophenol
V_{oc}	Open circuit voltage
wt	weight
ZnO	Zinc oxide
ZnPc	Zinc phthalocyanine
ZnS	Zinc sulfide
ZrO_2	Zirconium dioxide
6PAA	6-palmitate ascorbic acid
η	Efficiency

References

[1] Becquerel E. C R Acad Sci Paris 1839;9:561.
[2] Perlin. From Space to Earth–The story of solar Electricity. Ann Arbor, MI: AATEC Publications; 1999.
[3] Sun S, Fan Z, Wang Y, Haliburton J. Organic solar cell optimization. J Mater Sci 2005;40:1429–43.
[4] Chapin DM, Fuller CS, Pearson GL. A new silicon p–n junction photo cell for converting solar radiation into electrical power. J Appl Phys 1954;25:676.
[5] Roberson LB, Poggi MA, Januszkowalik, Smestod GP, Bottomley LA, Tolbert LM. Correlation of morphology and device performance in inorganic – organic TiO_2 – polythiophene hybrid solar cells. Coord Chem Rev 2004;248:1491–7.
[6] Rohatgi A, Jeong JW. High efficiency screen printed silicon ribbon solar cells by effective defect passivation and rapid thermal processing. Appl Phys Lett 2003;82:224–9.
[7] Narashima S, Rohatgi A.In: Proceeding of the 26th IEEE PV specialists conference. 1997. p. 63.
[8] Arici E, Meissner D, Schaffler F, Sariciftci NS. Core/shell nano materials in photovoltaics. Int J Photoenergy 2003;5:199–208.
[9] Halls JJM, Walsh CA, Greenham NC, Marseglia EA, Friend RH, Moratti SC, et al. Efficient photodiodes from interpenetrating polymer networks. Nature 1995;376:450–98.
[10] Veenstra SC, Verhees WJH, Kroon JM, Koetse MM, Sweelssen J, Bastiaansen JJAM, et al. Photovoltaic properties of a conjugated polymer blend of MDMO-PPV and PCNEPV. Chem Mater 2004;16:2503–8.
[11] Yu G, Gao J, Hummelen JC, Wudl F, Heeger AJ. Polymer photovoltaic cells—enhanced efficiencies via a network of internal donor acceptor heterojunction. Science 1995;270:1789–91.
[12] Shaheen SE, Brabec CJ, Sariciftci NS, Padinger F, Fromherz T, Hummelen JC. 2.5% efficient organic plastic solar cells. Appl Phys Lett 2001;78:841–3.
[13] Schilinsky P, Waldauf C, Brabec CJ. Recombination and loss analysis in polythiophene based bulk heterojunction photodetector. Appl Phys Lett 2002;81:3885–7.
[14] Wienk MM, Kroom JM, Verhees WJH, Knol J, Hummelen JC, Van Hal PA, et al. Efficient methano[70]fullerene/MDMO-PPV bulk heterojunction photovoltaic cells. Angew Chem Int Ed 2003;42:3371.

[15] Huynh WU, Dittmer JJ, Alivisatos AP. Hybrid nanorod-polymer solar cells. Science 2002;295:2425–7.
[16] Sun B, Marx E, Greenham NC. Photovoltaic devices using blends of branched CdSe nanoparticles and conjugated polymers. Nano Lett 2006;3:961–3.
[17] Sun B, Snaith HJ, Dhoot AS, Westenhoof S, Greenham NC. Vertically segregated hybrid blends for photovoltaic devices with improved efficiency. J Appl Phys 2005;97:014914.
[18] Kwong CY, Djurisic AB, Chui PC, Cheng KW, Chan WK. Influence of solvent on film morphology and device performance of poly(3-hexylthiophene): TiO_2 nanocomposite solar cells. Chem Phys Lett 2004;384:372–5.
[19] Beek WJE, Wienk MM, Janssen RAJ. Efficient hybrid solar cells from zinc oxide nanoparticles and a conjugated polymer. Adv Mater 2004;16: 1009–13.
[20] Beek WJE, Wienk MM, Kemerink M, Yang X, Janssen RAJ. Hybrid zinc oxide conjugated polymer bulk heterojunction solar cells. J Phys Chem 2005;109: 9505–16.
[21] McDonald SA, Konstantatos G, Zhang S, Cyr PW, Klem EJD, Levina L, et al. Solution-processed PbS quantum dot infrared photo detectors and photovoltaics. Nat Mater 2005;4:138–42.
[22] Watt AAR, Blake D, Warner JH, Thomson EA, Tavenner EL, Rubinsztein-Dunlop H, et al. Lead sulfide nanocrystal: conducting polymer solar cells. J Phys D Appl Phys 2005;38:2006–12.
[23] Qi D, Fischben M, Drndic M, Selmic S. Efficient polymer-nanocrystal quantum dot photo detectors. Appl Phys Lett 2005;86:093103.
[24] Choudhury KR, Sahoo Y, Ohulchansky TY, Prasad PN. Efficient photoconductive devices at infrared wavelengths using quantum dot – polymer nanocomposites. Appl Phys Lett 2005;87:073110.
[25] Arici E, Sariciftci NS, Meissner D. Hybrid solar cell based on nano particles of $CuInS_2$ in organic matrices. Adv Funct Mater 2003;13:165–71.
[26] Arici E, Hoppe H, Schaffler F, Meissner D, Malik MA, Sariciftci NS. Morphology effects in nanocrystalline $CuInSe_2$ – conjugated polymer hybrid systems. Appl Phys A Mater Sci Process 2004;79:59–64.
[27] Coakley K, McGehee MD. Photovoltaic cells made from conjugated polymers infiltrated into mesoporous titania. Appl Phys Lett 2003;83:3380–2.
[28] Coakley K, Liu Y, McGehee MD, Frindell KL, Stucky GD. Infiltrating semiconducting polymers into self-assembled mesoporous titania films for photovoltaic applications. Adv Funct Mater 2003;13:301–6.
[29] Ravirajan P, Haque SA, Durrant JR, Bradley DDC, Nelson J. The effect of polymer optoelectronic properties on the performance of multilayer hybrid polymer/ TiO_2 solar cells. Adv Funct Mater 2005;15:609–18.
[30] Bartholomew GP, Heeger AJ. Infiltration of regioregular poly[2,2′-(3-hexylthiophene)] into random nanocrystalline TiO_2 networks. Adv Funct Mater 2005;15:677–82.
[31] Ravirajan P, Bradley DDC, Nelson J, Haque SA, Durrant JR, et al. Efficient charge collection in hybrid polymer/TiO_2 solar cells using poly(ethylenedioxythiophene)/polystyrene sulphonate as a hole collector. Appl Phys Lett 2005;86: 143101.
[32] Wang H, Oey CC, Djurisic AB, Xie MH, Leung YH. Titania bicontinuous network structures for solar cell applications. Appl Phys Lett 2005;87:023507.
[33] Arici E, Serdar Sariciftci N, Meissner D. Hybrid solar cells based on nanoparticles of $CuInS_2$ in organic matrices. Adv Funct Mater 2003;13:165–71.
[34] Arici E, Hoppe H, Schaffler F, Meissner D, Malik MA, Sariciftci NS. Morphology effects in nanocrystalline CuInSe2-conjugated polymer hybrid systems. Appl Phys A 2004;79:59–64.
[35] Liu J, Tanaka T, Sivula K, Paul Alivisatos A, Frechet JMJ. Employing end functional polythiophene to control the morphology of nanocrystal-polymer composites in hybrid solar cells. J Am Chem Soc 2004;126:6550–1.
[36] Beek WJE, Slooff LH, Wienk MM, Kroon JM, Janssen RAJ. Hybrid solar cells using a zinc oxide precursor and a conjugated polymer. Adv Funct Mater 2005;15:1703–7.
[37] Slooff LH, Kroon JM, Loos J, Koetse MM, Sweelssen J. Influence of the relative humidity on the performance of polymer/TiO_2 photovoltaic cells. Adv Funct Mater 2005;15:689–94.
[38] Stakhira PY, Vertsimaha YaI, Aksimentyeva OI, Cizh BR. Hybrid solar cells based on dispersed InSe-polyaniline composites. Phys Chem Solid State 2005;6:96–8.
[39] Watt AAR, Blake D, Warner JH, Thomsen EA, Tavenner EL, Rubinsztein-Dunlop H, et al. Lead sulfide nanocrystal: conducting polymer solar cells. J Phys D Appl Phys 2005;38:2006–12.
[40] Lin Y-J, Wang L, Chiu W-Y. Novel poly(3-methylthiophene)-TiO_2 hybrid materials for photovoltaic cells. Thin Solid Films 2006;511–512:199–202.
[41] Gunes S, Neugebauer H, Sariciftci NS, Roither J, Kovalenko M, Pillwein G, et al. Hybrid solar cells using HgTe nanocrystals and nanoporous TiO_2 electrodes. Adv Funct Mater 2006;16:1095–9.
[42] Beek WJE, Wienk MM, Janssen RAJ. Hybrid solar cells from regioregular polythiophene and ZnO nanoparticles. Adv Funct Mater 2006;16:1112–6.
[43] Choi S-H, Song H, Park IK, Yum J-H, Kim S-S, Lee S, et al. Synthesis of size controlled CdSe quantum dots and characterization of CdSe-conjugated polymer blends for hybrid solar cells. J Photochem Photobiol A Chem 2006;179:135–41.
[44] Zhou Y, Li Y, Zhong H, Hou J, Ding Y, Yang C, et al. Hybrid nanocrystal/polymer solar cells based on tetrapod-shaped dSe_xTe_{1-x} nanocrystals. Nanotechnology 2006;17:4041–7.
[45] Han L, Qin D, Jiang X, Liu Y, Wang L, Chen J, et al. Synthesis of high quality zinc-blende CdSe nanocrystals and their application in hybrid solar cells. Nanotechnology 2006;17:4736–42.
[46] Koster LJA, van Strien WJ, Beek WJE, Blom PWM. Device operation of conjugated polymer/zinc oxide bulk heterojunction solar cells. Adv Funct Mater 2007;17:1297–302.
[47] Kim S-S, Jo J, Chun C, Hong J-C, Kim D-Y. Hybrid solar cells with ordered TiO_2 nanostructures and MEH-PPV. J Photochem Photobiol A Chem 2007;188: 364–70.
[48] Moet DJD, Anton Koster L, de Boer B, Blom PWM. Hybrid polymer Solar cell from highly reactive diethylzinc: MDMO-PPV versus P3HT. Chem Mater 2007;19:5856–61.
[49] Wang L, Liu YS, Jiang X, Qin DH, Cao Y. Enhancement of photovoltaic characteristics using a suitable solvent in hybrid polymer/multiarmed CdS nanorods solar cells. J Phys Chem C 2007;111:9538–42.
[50] Wang Z, Qu S, Zeng X, Zhang C, Shi M, Tan F, et al. Synthesis of MDMO-PPV capped PbS quantum dots and their application to solar cells. Polymer 2008;49:4647–51.
[51] Yan L, YanBing H, Hui J, QuanMin S, Yan W, ZhiHui F. Photovoltaic properties of MEH-PPV/TiO_2 nanocomposites. Chin Sci Bull 2008;53:2743–7.
[52] Suresh P, Balaraju P, Sharma SK, Roy MS, Sharma GD. Photovoltaic devices based on PPHT:ZnO and dye-sensitized PPHT:ZnO thin films. Sol Energy Mater Sol Cells 2008;92:900–8.
[53] Wang M, Wang X. PPV/TiO_2 hybrid composites prepared from PPV precursor reaction in aqueous media and their application in solar cells. Polymer 2008;49:1587–93.
[54] Vandewal K, Goris L, Haeldermans I, Nesladek M, Haenen K, Wagner P, et al. Fourier-transform photocurrent spectroscopy for a fast and highly sensitive spectral characterization of organic and hybrid solar cells. Thin Solid Films 2008;516:7135–8.
[55] Chang Y-M, Su W-F, Wang L. Photoactive polythiophene: titania hybrids with excellent miscibility for use in polymer photovoltaic cells. Macromol Rapid Commun 2008;29:1303–8.
[56] Krebs FC, Thomann Y, Thomann R, Andreasen JW. A simple nanostructured polymer/ZnO hybrid solar cell-preparation and operation in air. Nanotechnology 2008;19:424013 (1–12).
[57] Hau SK, Yip H-L, Baek NS, Zou J, O'Malley K, Jen AKY. Air-stable inverted flexible polymer solar cells using zinc oxide nanoparticles as an electron selective layer. Appl Phys Lett 2008;92:253301 (1–3).
[58] Haeldermans I, Vanderwal K, Oosterbaan WD, Gadisa A, D'Haen J, Van Bael MK, et al. Ground-state charge-transfer complex formation in hybrid poly(3-hexyl thiophene): titanium dioxide solar cells. Appl Phys Lett 2008;93:223302. (1–3).
[59] Boucle J, Chyla S, Shaffer MSP, Durrant JR, Bradley DDC, Nelson J. Hybrid bulk heterojunction solar cells based on blends of TiO_2 nanorods and P3HT. C R Phys 2008;9:110–2.
[60] Gunes S, Marjanovic N, Nedeljkovic JM, Sariciftci NS. Photovoltaic characterization of hybrid solar cells using surface modified TiO_2 nanoparticles and poly(3-hexyl) thiophene. Nanotechnology 2008;19:424009 (1–5).
[61] Liu J, Wang W, Yu H, Wu Z, Peng J, Cao Y. Surface ligand effects in MEH-PPV/ TiO_2 hybrid solar cells. Sol Energy Mater Sol Cells 2008;92:1403–9.
[62] Qiao Q, Xie Y, McLeskey Jr JT. Organic/inorganic polymer solar cells using a buffer layer from all-water-solution processing. J Phys Chem C 2008;112: 9912–6.
[63] Bredol M, Matras K, Szatkowski A, Sanetra J, Prodi-Schwab A. P3HT/ZnS: a new hybrid bulk heterojunction photovoltaic system with very high open circuit voltage. Sol Energy Mater Sol Cells 2009;93:662–6.
[64] Zeng T-W, Lo H-H, Chang C-H, Lin Y-Y, Chen C-W, Su W-F. Hybrid poly(3-hexylthiophene)/titanium dioxide nanorods material for solar cell applications. Sol Energy Mater Sol Cells 2009;93:952–7.
[65] Chen L-C, Wang C-C, Cheng C-B. Influence of dopant and polymeric matrix on indium tin oxide/p-zinc phtalocyanine/n-Si hybrid solar cells. Thin Solid Films 2009;517:1790–3.
[66] Wu M-C, Lo H-H, Liao H-C, Chen S, Lin Y-Y, Yen W-C, et al. Using scanning probe microscopy to study the effect of molecular weight of poly(3-hexylthiophene) on the performance of poly(3-hexylthiophene):TiO_2 nanorod photovoltaic devices. Sol Energy Mater Sol Cells 2009;93:869–73.
[67] Wu M-C, Liao H-C, Lo H-H, Chen S, Lin Y-Y, Yen W-C, et al. Nanostructured polymer blends (P3HT/PMMA): inorganic titania hybrid photovoltaic devices. Sol Energy Mater Sol Cells 2009;93:961–5.
[68] Yun D, Feng W, Wu H, Yoshino K. Efficient conjugated polymer-ZnSe and -PbSe nanocrystals hybrid photovoltaic cells through full solar spectrum utilization. Sol Energy Mater Sol Cells 2009;93:1208–13.
[69] Wang Z, Qu S, Zeng X, Liu J, Zhang C, Tan F, et al. The application of SnS nanoparticles to bulk heterojunction solar cells. J Alloys Compd 2009;482:203–7.
[70] Wang Z, Qu S, Zeng X, Liu J, Zhang C, Shi M, et al. The synthesis of MDMO-PPV capped PbS nanorods and their application in solar cells. Curr Appl Phys 2009;9:1175–9.
[71] Liu C-Y, Holman ZC, Kortshagen UR. Hybrid solar cells from P3HT and silicon nanocrystals. Nano Lett 2009;9:449–52.
[72] Chou C-Y, Huang J-S, Wu C-H, Lee C-Y, Lin C-F. Lengthening the polymer solidification time to improve the performance of polymer/ ZnO nanorod hybrid solar cells. Sol Energy Mater Sol Cells 2009;93: 1608–12.
[73] Kalita G, Adhikari S, Aryal HR, Afre R, Soga T, Sharon M, et al. Silicon nanowire array/polymer hybrid solar cell incorporating carbon nanotubes. J Phys D Appl Phys 2009;42:115104 (1–5).

[74] Lin Y-Y, Wang D-Y, Yen H-C, Chen H-L, Chen C-C, Chen C-M, et al. Extended red light harvesting in a poly(3-hexylthiophene)/iron disulfide nanocrystal hybrid solar cell. Nanotechnology 2009;20:405207 (1–5).
[75] Verma D, Ranga Rao A, Dutta V. Surfactant-free CdTe nanoparticles mixed MEH-PPV hybrid solar cell deposited by spin coating technique. Sol Energy Mater Sol Cells 2009;93:1482–7.
[76] Takeda A, Oku T, Suzuki A, Kikuchi K, Kikuchi S. Fabrication and characterization of inorganic–organic hybrid solar cells based on $CuInS_2$. JCS-Japan 2009;117:967–9.
[77] Liu J, Wang S, Bian Z, Shan M, Huang C. Organic/inorganic hybrid solar cells with vertically oriented ZnO nanowires. Appl Phys Lett 2009;94:173107 (1–3).
[78] Svrcek V, Turkevych I, Kondo M. Photoelectric properties of silicon nanocrystals/P3HT bulk-heterojunction ordered in titanium dioxide nanotube arrays. Nanoscale Res Lett 2009;4:1389–94.
[79] Briseno AL, Holcombe TW, Boukai AI, Garnett EC, Shelton SW, Frechet JJM, et al. Oligo-and polythiophene/ZnO hybrid nanowire solar cells. Nano Lett 2010;10:334–40.
[80] Dayal S, Kopidakis N, Olson DC, Ginley DS, Rumbles G. Photovoltaic devices with a low band gap polymer and CdSe nanostructures exceeding 3% efficiency. Nano Lett 2010;10:239–42.
[81] Choudhury KR, Song DW, So F. Efficient solution-processed hybrid polymer-nanocrystal near infrared light-emitting devices. Org Electron 2010;11:23–8.
[82] Wang T-L, Yang C-H, Shieh Y-T, Yeh A-C, Juan L-W, Zeng HC. Synthesis of new nanocrystal-polymer nanocomposite as the electron acceptor in polymer bulk heterojunction solar cells. Eur Polym J 2010;46:634–42.
[83] Yan J, Sun C, Tan F, Hu X, Chen P, Qu S, et al. Electropolymerized poly(3,4-ethylenedioxythiophene):poly(styrene sulfonate) (PEDOT:PSS) film on ITO glass and its application in photovoltaic device. Sol Energy Mater Sol Cells 2010;94:390–4.
[84] Stylianakis MM, Mikroyannidis JA, Kymakis E. A facile, covalent modification of single-wall carbon nanotubes by thiophene for use in organic photovoltaic cells. Sol Energy Mater Sol Cells 2010;94:267–74.